

A theoretical investigation of conformational aspects of polymorphism. Part 2. Diarylamines



Jonathan Starbuck,[†] Robert Docherty,[‡] Michael H. Charlton and David Buttar

Zeneca Specialties Research Centre, Hexagon House, PO Box 42, Blackley, Manchester, UK M9 8ZS

Received (in Cambridge) 3rd December 1998, Accepted 16th February 1999

The crystal chemistry and torsional profiles of three polymorphic diarylamines have been compared and contrasted. Although they have similar potential energy surfaces (PESs) for the main rotatable bond, the torsional distribution of the observed polymorphs differs greatly. In particular there are reported crystal structures for some but not all of the molecules at various positions on the PES, some of which are either maxima or non-stationary points on the gas phase surface. We have explained the distribution of the observed torsion values and postulated new packing motifs based on those found in the other molecules. According to lattice energy calculations, some of these 'new polymorphs' are predicted to be more stable than those reported in the literature.

1 Introduction

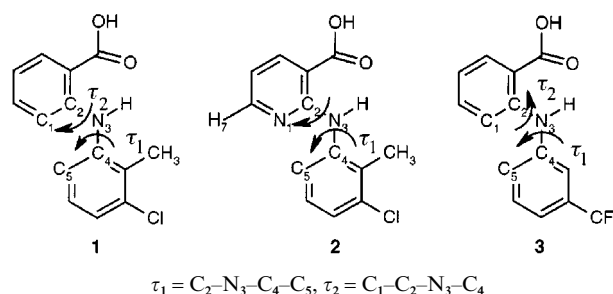
The energies involved in rotating about single bonds are comparable to the lattice energy differences observed between polymorphs and so it is not surprising that molecules which possess torsional degrees of freedom often exhibit different conformational forms in the solid state.¹⁻³ However, we have previously reported a case for which the calculated gas phase energy difference between the crystallographic conformations is of the order of 10 kcal mol⁻¹.⁴ This conformational energy difference is significantly higher than any found in previous studies.⁵ It is also larger than the value generally accepted as the maximum energy that can be supplied by the crystal lattice to stabilise an unstable conformation. For this particular system, the total (lattice + conformational) energy difference between two observed polymorphs was about 6 kcal mol⁻¹, a fact that has important implications for those interested in the prediction of crystal structures and structure determination from X-ray powder diffraction data.

The solid state structural arrangement(s) adopted by a molecule will depend upon the subtle equilibrium between the intra- and intermolecular interactions achievable within particular packing arrangements. The conformations found in the solid state will be dependent on the gas phase potential energy surface (PES) and on solid state packing considerations. They do not have to lie at minima on the gas phase PES, but they must be at a minimum on the solid state PES. In addition, solid state conformations might be expected to lie energetically and geometrically close to minima in the phase from which the crystals are produced. However, in our previous study of this field, we found that one of the known polymorphs of *o*-acetamidobenzamide lies very close to a gas phase minimum, whilst the other has torsions that differ by about 20°, as determined by large basis set *ab initio* calculations.⁴ Such differences could cause problems in crystal structure prediction techniques that employ a rigid (gas phase generated) probe to generate the initial packing motif.

In this study, we have used methodologies developed previously to examine three polymorphic diarylamine systems which are closely related in chemical structure. Our aims were to link

the molecular structures and conformational preferences to the observed polymorphic behaviour of these systems. Specifically to: (i) Investigate and compare the gas phase PESs for these molecules at various levels of theory; (ii) Map the solid state conformations onto these surfaces and examine the geometric and energetic differences between observed solid state conformations and those found in the gas phase. These differences are important as gas phase structures are used as the input to crystal structure prediction techniques; (iii) Study the PES to discover if any low-lying minima are not associated with observed crystal structures. These minima would make prime candidates for conformations for input into crystal structure prediction routines and may lie close to as yet undiscovered polymorphs; (iv) Investigate the relationship between observed conformations and polymorph occurrence; (v) To postulate the existence of novel polymorphs based on exchanging important conformations of some of the molecules with observed packing motifs of the others; (vi) Use the results to investigate the generally accepted maximum energy difference between polymorphs (<3 kcal mol⁻¹ for lattice energies or <1 kcal mol⁻¹ for total energies).^{6,7} These values are commonly used in polymorph prediction methods as a limit for the selection of potential polymorphs; (vii) Determine if semi-empirical and force field calculations are capable of reproducing conformations and energetics generated with good quality HF MO calculations; (viii) Relate the observed torsions seen in our molecules to the conformations found in similar compounds in the Cambridge Structural Database (CSD).⁸

The three molecules studied in this paper are: *N*-(3-chloro-2-methylphenyl)anthranilic acid⁹ **1** (CSD refcodes KAXXAI, KAXXAI01), 2-(2-methyl-3-chloroanilino)nicotinic acid¹⁰ **2** (BIXGIY, BIXGIY02, BIXGIY03) and 2-[[3-(trifluoromethyl)phenyl]amino]benzoic acid **3** (FPAMCA¹¹, FPAMCA11¹²).



[†] Current address: School of Chemistry, University of Bristol, Cantock's Close, Bristol, UK BS8 1TS.

[‡] Current address: Pfizer Central Research, Sandwich, Kent, UK CT13 9NJ.

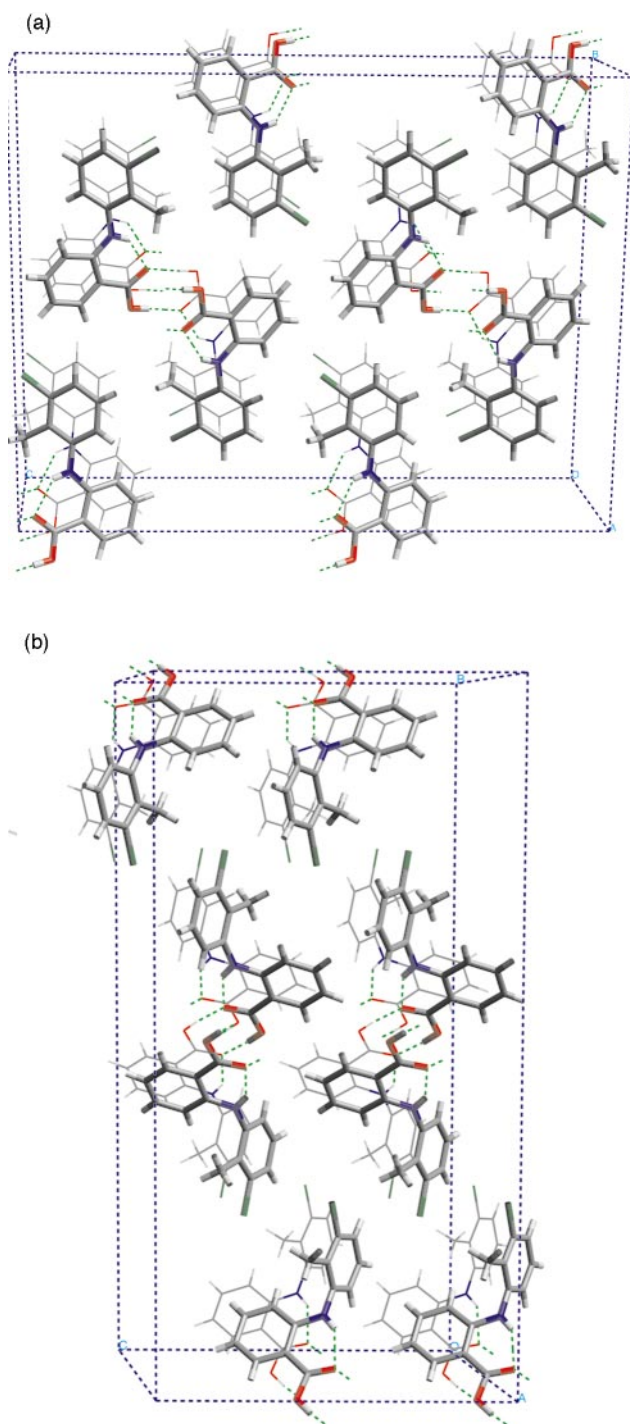


Fig. 1 View of the crystal packing of KAXXAI: (a) form I and (b) form II.

These molecules are similar in chemical structure but have different numbers of polymorphs published in the literature. The selected polymorphs differ in rotation about two common bonds, and might be expected to have similar rotation profiles.

Tolfenamic acid **1** is a potent anti-inflammatory drug. It has been observed to crystallise in two distinct forms, each with a different conformation. These are designated forms I (KAXXAI) and II (KAXXAI01) which are yellow and white, respectively.⁹ The two polymorphs form inversion related hydrogen bonded dimers, as frequently observed for carboxylic acid containing molecules. The intermolecular hydrogen bond distances are 1.71 (I) and 1.69 (II) whilst the intramolecular N–H···O contacts are 1.96 (I) and 2.02 Å (II). Fig. 1(a) and (b) show the view down the *a*-axis for forms I and II, respectively.

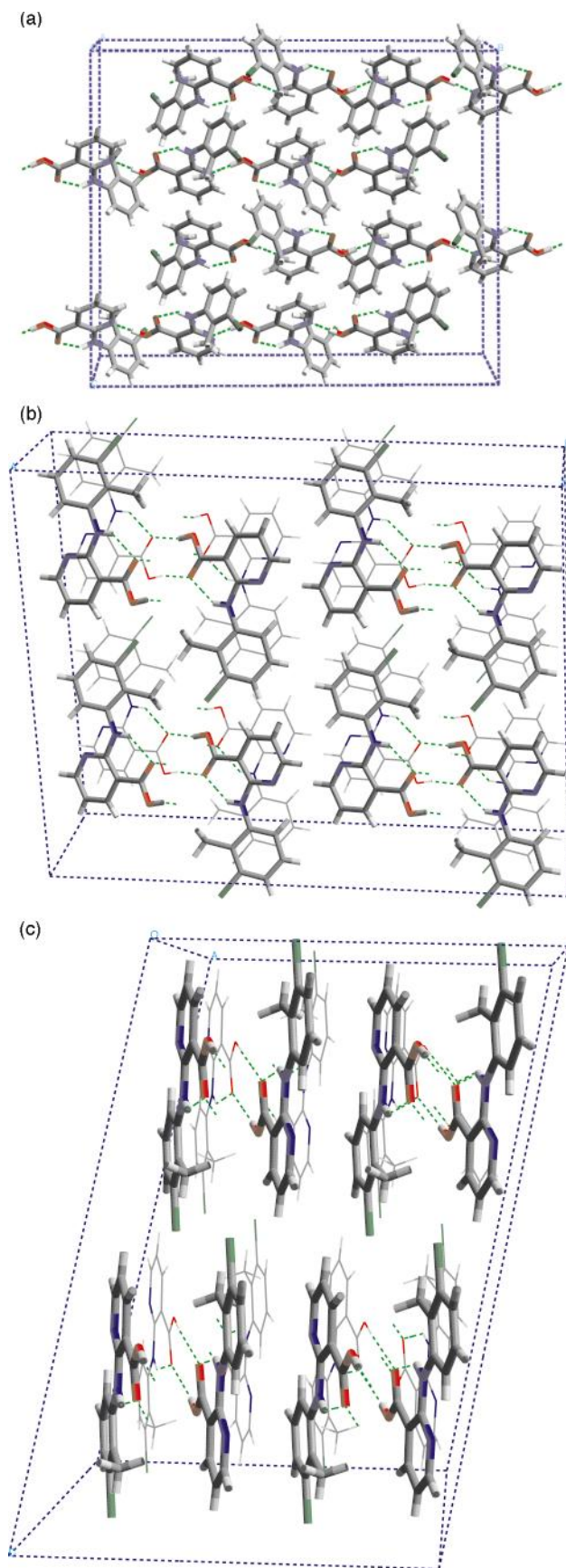


Fig. 2 View of the crystal packing of BIXGIY: (a) form I, (b) form III and (c) form IV.

Inter- and intramolecular hydrogen bonding is indicated by the dashed green lines. Thick lines are used to represent molecules at the front of picture, whilst those at the back are thinner. The dashed blue lines represent the extent of a 2 by 1 by 2 unit cell

Table 1 Crystal structure details

CSD Refcode	KAXXAI	KAXXAI01	BIXGIY	BIXGIY02	BIXGIY03	FPAMCA	FPAMCA11
Form	I	II	I	III	IV	I	II
<i>R</i> factor	0.029	0.052	0.052	0.070	0.048	0.049	0.074
<i>Z</i>	4	4	4	2	2	8	4
Space group	<i>P</i> 2 ₁ / <i>n</i>	<i>P</i> 2 ₁ / <i>c</i>	<i>P</i> 2 ₁ / <i>c</i>	<i>P</i> $\bar{1}$	<i>P</i> $\bar{1}$	<i>C</i> 2/ <i>c</i>	<i>P</i> 2 ₁ / <i>c</i>
<i>a</i> /Å	3.836	4.826	7.625	13.810	7.670	39.848	12.523
<i>b</i> /Å	21.997	32.128	14.201	3.858	7.254	5.107	7.868
<i>c</i> /Å	14.205	8.041	11.672	10.984	10.882	12.240	12.874
α /°	90	90	90	94.98	100.66	90	90
β /°	94.11	104.88	101.65	94.42	102.02	92.47	95.20
γ /°	90	90	90	95.57	86.97	90	90
<i>V</i> /Å ³	1196	1205	1238	578	582	2489	1263
<i>D</i> _x /Mg m ^{-3a}	1.450	1.443	1.410	1.510	1.500	—	1.470
<i>D</i> _M /Mg m ^{-3b}	1.453	1.442	1.409	1.509	1.499	1.501	1.479
τ_1 /°	±42.2	±107.7	±111.9	±22.2	±0.6	±176.5	±53.9
τ_2 /°	±8.0	±0.5	±3.2	±0.7	±1.1	±37.1	±1.8
Inter H-Bond/Å	1.715	1.686	1.610	1.703	1.756	1.720	1.793
Intra H-Bond/Å	1.962	2.018	1.858	1.996	1.913	2.017	1.979

^a Experimental density (computed from unit cell). ^b Measured density.

array. Inspection of the structure surrounding the dimers reveals no particularly short intermolecular contacts between molecules. Further details of the structures are given in Table 1. The conformational differences between the two crystal structures can be described by the torsion angles (τ_1 , τ_2), which have experimental values of (42, 8) (I) and (108, -1)° (II). In both forms, the carboxy group, the NH group, and C₄ all lie almost in the plane of the upper (carboxy-substituted) ring (in the orientation shown), *i.e.* $\tau_2 \approx 0$. The planarity is due to the intramolecular hydrogen bond between the carbonyl oxygen and the amine hydrogen, which is likely to be difficult to break during a rotation. However, this torsion (τ_2) is considered in the rotational profiles presented in this work to give consistency with structure 3.

BIXGIY, 2 is an analgesic and anti-inflammatory agent and has been characterised in four different crystal forms. One of these structures exists as a zwitterion, and is not considered here due to the difficulties in comparing force field (FF) energies for systems in which the electrostatics vary considerably. The remaining three structures show considerable variation in colour,¹⁰ and are designated forms I, III and IV (CSD refcodes BIXGIY, BIXGIY02 and BIXGIY03, respectively). Once again, the carboxy group, N₃ and C₄ of the molecule lie within 3° of the plane of the pyridyl ring. The major conformational difference between the three forms is the degree by which the phenyl ring is twisted from this plane about the N₃-C₄ bond as defined by τ_1 . Details of the structures of the three forms are given in Table 1.

The packing of this material is more complex than that observed for KAXXAI. The packing of forms I, III and IV is shown in Figs. 2(a) (1 by 2 by 2 unit cells), 2(b) (2 by 2 by 2 unit cells) and 2(c) (2 by 2 by 2 unit cells). In form I, the molecules pack such that chains are formed along the *b*-axis, held by a short O-H...N contact (1.61 Å) and a C-H...O contact (2.30 Å). Although these contacts are short for both traditional and special hydrogen bonds respectively,³ it is perhaps surprising that this motif is preferred to the conventional hydrogen bonding dimer arrangements observed in forms III and IV. In these two forms, the hydrogen bonds are 1.70 and 1.76 Å, respectively. The carboxylic acid dimers in form III are held together in the *ab* direction by a pair of C-H...N interactions (2.77 and 2.87 Å). A similar contact is present in form IV (2.74 Å). Once again, there are strong intramolecular N-H...O hydrogen bonds from the amino nitrogen in all three forms, with O...H distances of 1.86, 2.00 and 1.91 Å for forms I, III and IV, respectively.

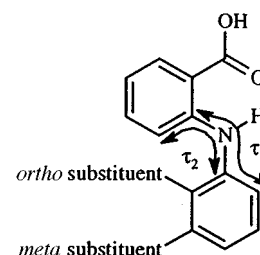
FPAMCA (or flufenamic acid), 3, is one of a series of compounds that have been shown to exhibit anti-pyretic and anti-inflammatory activity.¹² It is known to crystallise in several

different forms, of which two have been fully solved. These are designated I (FPAMCA¹¹) and II (FPAMCA11¹²), with different conformers in the two polymorphs. Details of the structures of both forms are given in Table 1. In both I and II, pairs of centrosymmetrically related molecules are connected by hydrogen bonds (1.72 and 1.79 Å respectively) between the carboxylic acid groups, as shown in Fig. 3(a) and (b). The dashed blue lines represent a 1 by 2 by 2 array [Fig. 3(a)] and a 2 by 1 by 2 array [Fig. 3(b)] of unit cells. As in molecules 1 and 2, the geometry around the nitrogen atom is planar in both forms due to N-H...O hydrogen bonds at distances of 2.02 and 1.98 Å. Form I of this molecule is the only example in this set in which τ_2 is not planar.

2 Methodology

2.1 Conformational preferences in the crystalline state

As described in our previous paper⁴ it is not unusual for observed solid state conformations to differ from those determined by theoretical gas phase calculations. It is therefore useful to supplement theoretical calculations with an examination of the conformational preferences observed in the crystalline state. There are a number of other diarylamines in the CSD that have not been included in the main study because there is only one polymorph of these in the database. All compounds selected were defined in the CSD as being 'organic'. They were located using a CSD search for two aromatic rings joined by an acyclic N-H group. All the ring atoms were allowed to be either carbon or nitrogen. One of the rings was substituted with a carboxy group in which the C-O bonds could be any bond type. The hits were exported into Sybyl v6.3¹³ and the torsions measured, as defined in Scheme 1. The substitution pattern



Scheme 1

was determined by the position of the substituent closest to the N-H group. It should be noted that in the unsubstituted systems, (lower ring = phenyl) τ_1 is ambiguously defined, due to the symmetry of this group. In these cases, the lowest torsional value has been used.

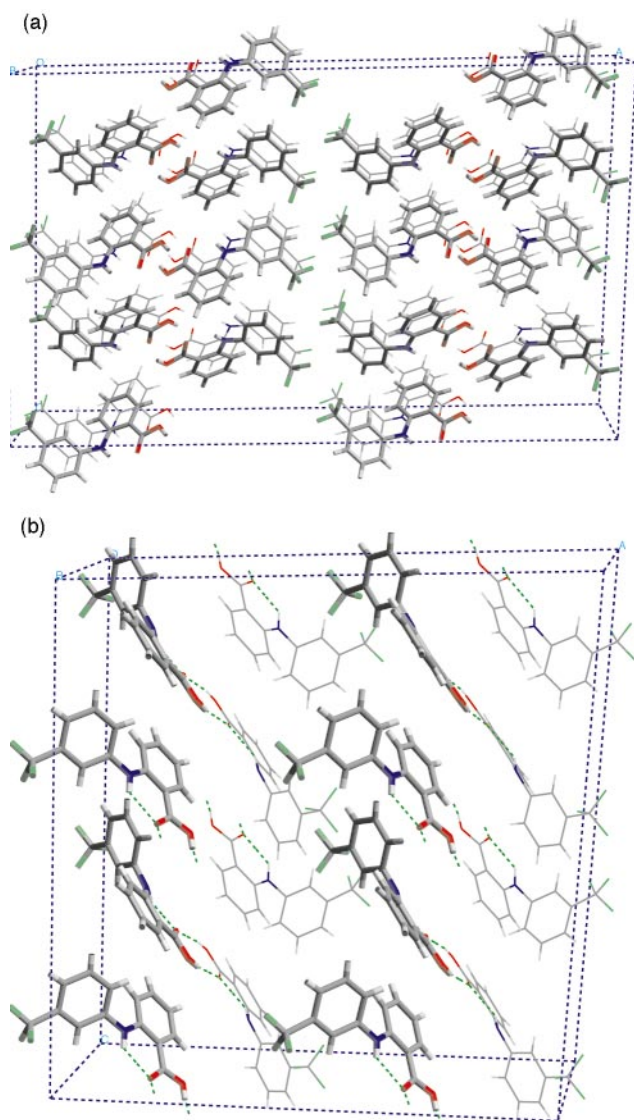


Fig. 3 View of the crystal packing of FPAMCA: (a) form I and (b) form II.

2.2 Conformational energies

Different theoretical methods can give very different representations of rotational profiles.⁴ It is probably necessary to use large basis set *ab initio* calculations to obtain reliable answers. As in our previous study, we have investigated a number of methodologies, comparing rapid FF calculations through to expensive HF studies. In large systems, the former are the best we can hope to apply, so it is important that we understand the limitations of the methods. The application of a range of computational tools gives some confidence if we obtain a general consensus in the results.

To evaluate the energy differences between conformers, the MOPAC 93 semi-empirical molecular orbital program¹⁴ was used to calculate AM1¹⁵ and PM3¹⁶ heats of formation for the structures. *Ab initio* studies using the GAMESS-UK¹⁷ program were also performed to calculate the difference in energies between conformations. Tripos FF energies were calculated using Sybyl and Dreiding¹⁸ values were computed using Cerius2 v3.5.¹⁹

We have already shown that single point calculations on each polymorph ($\Delta H_f^{\text{cryst}}$) give a poor measure of relative energy.⁴ Slight differences in the experimental bond lengths and angles between each polymorphic form, as well as between the crystal structures and theoretically calculated gas phase structures, introduce a methodological bias which affects the energy

difference calculations in an unpredictable way. Therefore, to study the conformational energy differences, we suggested evaluating the energies in a number of ways. In particular, we obtained reasonable conformational energy differences from structures in which only the hydrogen atoms were allowed to optimise (ΔH_f^1), structures in which all degrees of freedom were optimised apart from the torsions under study (ΔH_f^4) and from full optimisations to the nearest minimum (ΔH_f^5). For completeness, we also quote values for ΔH_f^2 and ΔH_f^3 , as described in the previous study.⁴

As more degrees of freedom were allowed to optimise, the final structures became less and less like the conformations found in the solid state. Energy differences calculated on conformations that differ significantly from those in the solid state may give differences in energy that are unrepresentative of the crystal. Thus, we devised a further method of evaluating the conformational energy difference using structures that were as close to those found in the crystal as possible, but in which this 'methodological energy bias' was removed. This involved FF optimisation of a single molecule within a cluster whilst the outside of the cluster itself was frozen in the configuration found in the crystal. This methodology gave energy differences very close to those found with the methods mentioned previously and is employed again here and is termed ΔH_f^6 .

FF calculations have limited accuracy and applicability but have the advantage of being relatively computationally efficient and allowing the study of molecules with hundreds of atoms. To some extent, the same may also be true of semi-empirical calculations. To be sure of the accuracy of the predictions made with these methods, it is advisable to validate the results with experimental information or high quality theoretical results. It has already been shown that the 3-21G basis set is not always sufficient to give reliable results,⁴ thus we have also used the larger, polarised 6-31G** basis set. Complete studies of the *ab initio* PES are not possible on this size of molecule due to the time required. Therefore, we have been limited to evaluating the differences between energies of partially optimised structures with two torsions frozen which are equivalent to the differences between ΔH_f^4 values and differences between two fully optimised energies which relate to the ΔH_f^5 results.

We have also evaluated the Tripos and Dreiding force field energy differences for the minima nearest to the observed crystal structures. To ensure that hydrogen bonding effects are reliably reproduced, we have included electrostatic terms in the force field. These were evaluated using AM1 charges (determined from the diagonal elements of the density matrix) calculated at the individual crystal geometries of each polymorph. This leads to differences in charges between the various conformational forms. AM1 charges have been chosen in this case because they are easily calculated and are consistent with the lattice energy calculations reported in this work.

2.3 Torsional scans

As well as studying the energetics of known polymorphs, we would also like to be aware of other minima on the PES which might correspond to as yet unreported polymorphs. To do this, we need to investigate the PES for all the important torsions using conformational search routines. For each molecule, we have defined the torsion angles that describe the differences between the conformations observed in the crystal structures. The conformational space was searched using the Tripos FF in 10° steps from -180 to 180° for both torsions. At each point of the scan, all other geometrical parameters were allowed to relax. This was repeated with AM1 and PM3 using 15° steps and the MOPAC in-built torsional search methodology was used with the EF minimiser²⁰ to optimise each point on the PES to a gradient norm of less than 1.0. The torsional search methodology speeds up the calculations by making a small change to the optimised geometry of the previous point on the

PES, and using this as the starting structure for the next point. This can have the disadvantage of introducing slight asymmetries in surface features, depending on which direction they are approached from, unless very low optimisation cut-offs are used, which is very time-consuming.

Surface maps have been generated for the two-dimensional scans using the GMT program.²¹ The shape of these surfaces are dependent upon the search methodology employed, the choice of starting structure and z -matrix ordering as well as the grid density and interpolation used to generate smooth surfaces. The plots give a general guide to the conformational PES, but regions of special interest have been thoroughly investigated with full optimisations. At certain locations on the PES involving significant steric clash, the Tripos minimiser failed to bring the energy down close to that of nearby regions, giving unrealistically large peaks on the surface maps. To avoid changing the energy scale to cover a large enough range to include these points, the energy values have been truncated. These points are shown in white on the force field maps.

2.4 Lattice energy calculations

The HABIT95²² and Cerius2 (v3.5) programs were used to evaluate the solid state energy differences between polymorphs.²³ These lattice energy calculations have been performed using the Dreiding and Tripos FFs which are general molecular mechanics FFs, not specifically derived for crystal packing studies. However, they provide consistency with the conformational calculations and have proved useful in previous studies.⁴ In addition, Dreiding is the FF used in certain polymorph prediction strategies.⁶ Again, AM1 charges calculated at the appropriate crystal structure geometry were used to evaluate the electrostatic part of the intermolecular energy. Dreiding calculations were also performed in which some minimisation of the packing was allowed. Unit cell parameters were fixed, but rigid body rotations and translations were allowed. In a second set of calculations, the unit cell parameters were also allowed to relax. These minimisations were performed to overcome the particular sensitivity of the Dreiding FF to hydrogen bond lengths in carboxylic acids.²⁴

3 Results

3.1 Experimentally observed conformational preferences of diarylamines

A graph of torsions τ_1 and τ_2 is plotted in Fig. 4 and colour-coded depending upon ring type (of the COOR substituted ring) and substitution pattern of the other ring. All compounds have either a phenyl or an *o*-pyridyl carboxy-substituted ring, except for TRFLOC10 (dark purple) which has a *p*-pyridyl carboxy-substituted ring. The effect on the two torsions in this compound would be expected to be similar to that of a phenyl ring.

A number of observations can be made from this plot. Most of the compounds only occupy a very narrow band of τ_2 values ($< \pm 25^\circ$). For τ_1 , most of the molecules can be found between 0 and 120° . High τ_1 values ($\sim 180^\circ$) are only seen in the *m*-substituted compounds (magenta and cyan), for which there is a noticeable distortion of τ_2 . None of the unsubstituted phenyl compounds lie in this region, yet sterically, they are very similar. *O*-Substituted phenyl compounds (red) cluster at $\tau_1 \sim 80^\circ$. The only completely planar compounds have the *o*-pyridyl ring (BIXGIY, green), for which steric repulsions between the two rings are likely to be small. Compounds with *o*-COOR groups in both rings (orange) have lower τ_1 and slightly higher τ_2 than the other *o*-phenyl molecules. Compound QQQBTY01 is particularly interesting because it has two molecules in the asymmetric unit, with τ_1 values of 46.6 and 110.0° .

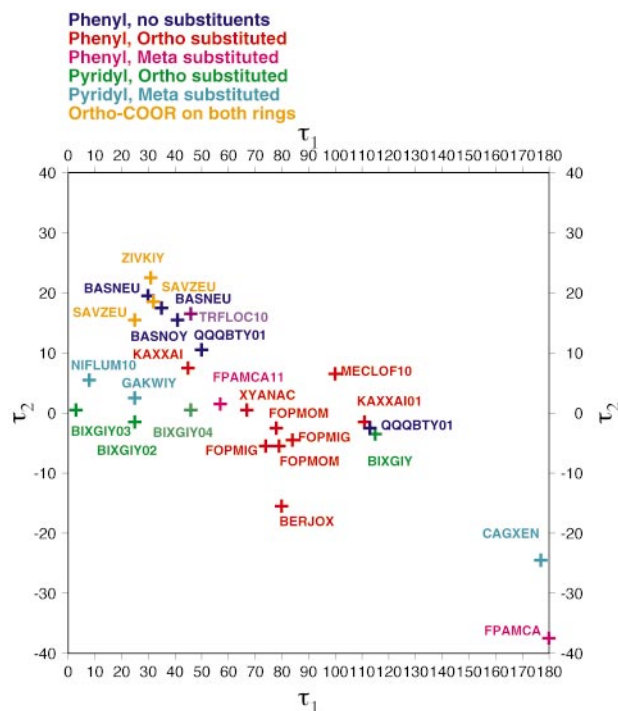


Fig. 4 Torsional distribution of diarylamines found in the CSD, colour-coded by ring type.

3.1 Torsional maps

The Tripos FF, AM1 and PM3 potential energy profiles are shown in Fig. 5(a), (b), (c) (KAXXAI), 6(a), (b), (c) (BIXGIY) and 7(a), (b), (c) (FPAMCA), respectively. The regions of interest on these maps are characterised later in this study.

3.1.1 KAXXAI. For KAXXAI, the AM1 and FF maps show a high degree of topographical similarity; both having the same low-lying region when τ_2 has a near-zero value. Two pairs of symmetry-related minima lie in this region according to the FF map, although only the more central of these appears on the AM1 map. This is the global minimum region. As τ_1 approaches $\pm 180^\circ$ (at near-zero values of τ_2), the energy rises noticeably above these minima. There is a maximum at (0,0) on both maps, which is noticeably higher in energy in the FF case.

At values of $|\tau_2| > 90^\circ$ on the FF map, the potential energy is at least 7 kcal mol^{-1} higher than the global minima, and rises to values much higher than this in places. There is one pair of minima evident in the $|\tau_2| > 90^\circ$ region of this map at roughly $(+/-140, +/-140)$ and second flat region at $(+/-30, +/-140)$. From the map, these are about 7 kcal mol^{-1} higher in energy than the global minima. The same regions would appear to be areas of low gradient (rather than minima) on the AM1 map. The two have different energies according to AM1, and are 10 and 7 kcal mol^{-1} less stable than the global minima, respectively.

The conformations found in the crystal structures are marked on the maps. In the FF case, both forms lie close to the global minima, although form II is slightly more stable. Form I lies close to the AM1 global minimum, but form II, although not significantly higher in energy, lies over 60° removed from the centre of the minimum, on a flat part of the PES. Thus, it is apparent that these two methods give results that are qualitatively different, although in only minor ways.

The PM3 map exhibits the same structural features as AM1 in the higher energy regions, although for some reason, the central region is considerably less symmetrical and very different in topology from the AM1 and FF maps. The nature of the PM3 PES at the observed conformations is not well defined. In one half of the map, form II lies close to a minimum, whilst its

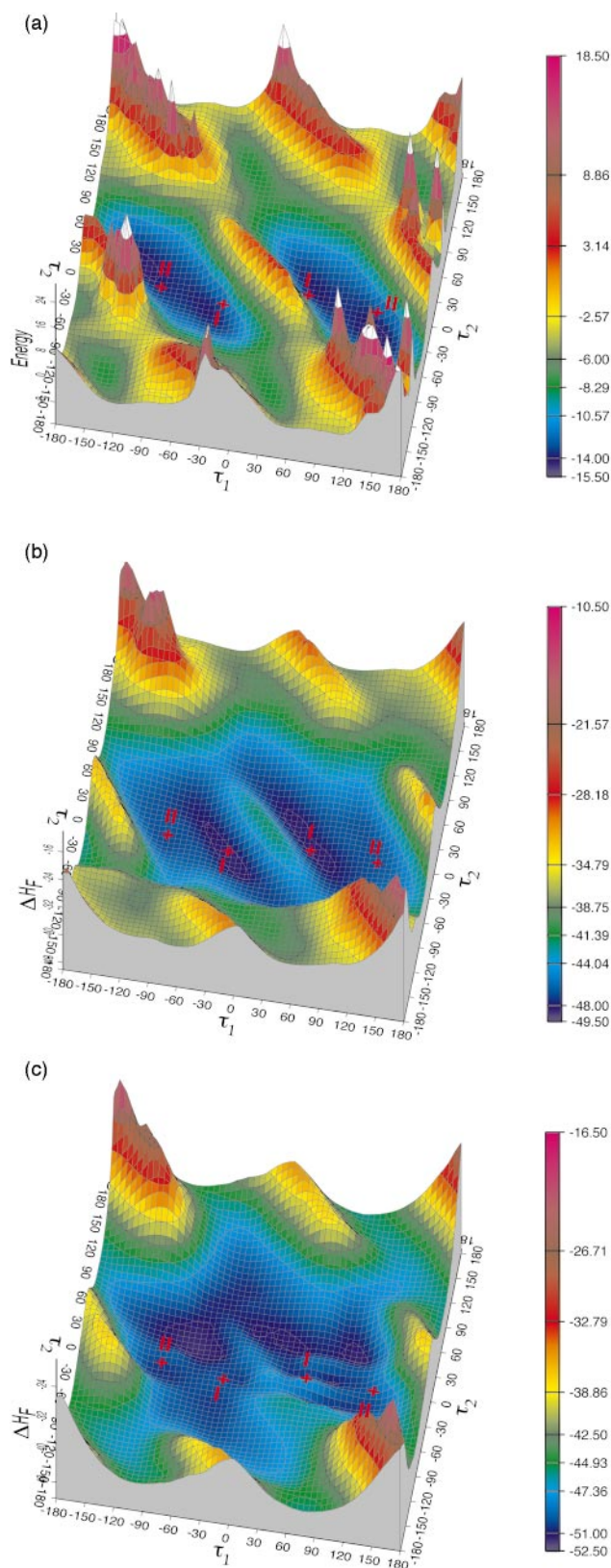


Fig. 5 (a) Force field, (b) AM1 and (c) PM3 potential energy surfaces for KAXXAI (energy in kcal mol⁻¹, torsions in degree). Roman numerals indicate the location of forms I and II.

symmetry-related equivalent has a very different topography. Because of concern over the lack of symmetry in the PM3 map, we re-ran the calculation with a gradient tolerance reduced to 0.05. This had a negligible effect on the PES.

3.1.2 BIXGIY. There is a high degree of similarity between the BIXGIY maps [Fig. 6(a), (b), (c)] and those for KAXXAI.

Again, we can see a low lying region when τ_2 is close to zero, with maxima in this region at $(0,0)^\circ$ and $(\pm 180,0)^\circ$. As before, the Tripos FF shows the global minimum consists of two pairs of symmetry-related minima. Again, only one pair is apparent on the AM1 map. The sudden shelf up to high energy values is also present when $|\tau_2| > 90^\circ$, and as before, there are two symmetry-related pairs of minima in this region, in the same positions as on the KAXXAI maps with energies about 7 kcal mol⁻¹ (FF) above the global minima. As before, these show up as flat regions or a very shallow minima on the AM1 map about 9 kcal mol⁻¹ ($-120, -120^\circ$) and 7 kcal mol⁻¹ ($25, -100^\circ$) above the global minima, respectively.

The conformations observed in the crystal structures are also marked on the maps. It is notable that form IV lies at the maximum at $(0,0)$, although this is only 5 kcal mol⁻¹ (FF) or 1.5 kcal mol⁻¹ (AM1) higher than the global minima. This is a considerably smaller difference than found for the equivalent conformation of KAXXAI. On the FF map, Form III lies between the maximum at $(0,0)$ and the global minimum [centred at $(-45,0)$], on a region of the PES that has a non-zero gradient and is about 3 kcal mol⁻¹ above the global minimum. Form I lies close to the centre of a second minimum. On the AM1 map, forms I and III lie slightly to either side of the global minima, and are slightly higher in energy.

As with KAXXAI, the PM3 map shows the same overall features as those observed with AM1, but the map is considerably less symmetrical in the low-lying regions. There is not an obvious maximum at the centre of the map, as located by the other methods. In our previous study PM3 appeared to have a preference for planar structures that were characterised as transition states with *ab initio* methods.⁴

3.1.3 FPAMCA. This is the only one of these three molecules that has a reported polymorph (form I) with a markedly non-planar value for τ_2 . Most of the features highlighted in the maps for BIXGIY and KAXXAI also occur in the FPAMCA maps [Fig. 7(a), (b), (c)]. This is the only case in which the AM1 map shows two separate global minima (neglecting the symmetry-related pairing at this point).

Forms I and II are marked on the PES maps. On the FF map, it can be seen that form II lies in the more central of the symmetry related minima. Form I is more removed from its nearest minimum (about 40° difference in τ_1) but is also only about 3 kcal mol⁻¹ above it. According to the AM1 map, form II lies very close to the central minimum, and form I lies near the centre of the other minimum that wraps from one side of the map to the other.

From the FF map, it is apparent that the molecule cannot be completely planar, as the potential energy surface has very large maxima where both τ_1 and τ_2 are equal to 0 or 180° . In contrast, the AM1 map suggests that there is a much smaller penalty for adopting some of the possible planar structures.

The PM3 map shows the same topographical features as AM1 in the higher energy regions, but as with the other two molecules, the scan fails to show the essential symmetry of the system.

3.2 Conformational energy studies: semi-empirical, force field and *ab initio* energy calculations

The semi-empirical heats of formation and force field energies along with the energy differences relative to the most stable form are shown for KAXXAI in Table 2. The equivalent results for BIXGIY and FPAMCA are given in Tables 3(a), 3(b) and 4, respectively. As we have found previously,⁴ single point energy calculations on the published crystal structures give an unreliable measure of both relative and absolute energies, and have only been included for consistency. It can be seen that allowing the positions of the hydrogen atoms to optimise (ΔH_f^1) relieves most but not all of this problem. The *ab initio* energies are reported in Table 5.

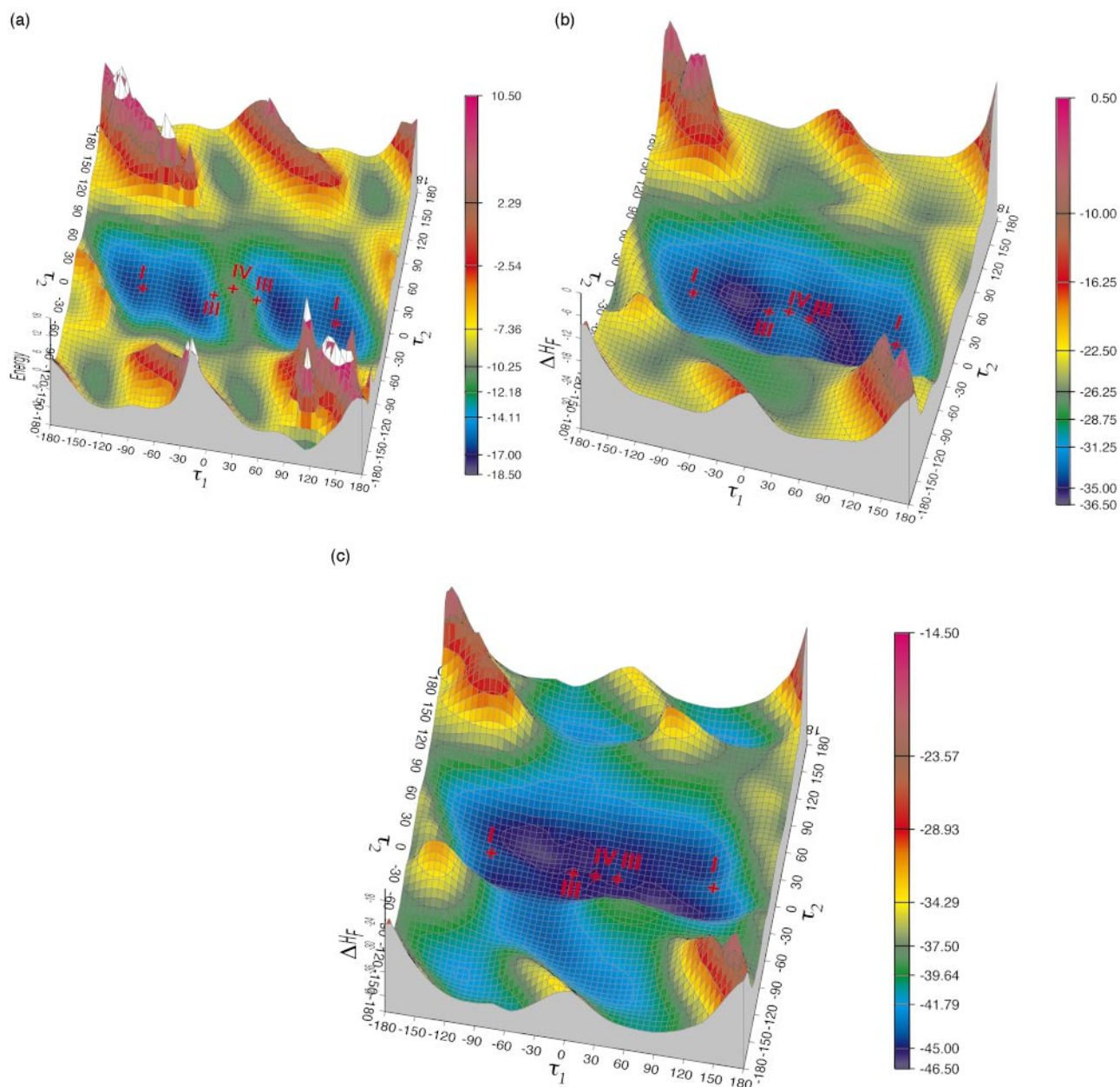


Fig. 6 (a) Force field, (b) AM1 and (c) PM3 potential energy surfaces for BIXGIY (energy in kcal mol⁻¹, torsions in degrees). Roman numerals indicate the location of forms I, III and IV.

Table 2 Semi-empirical heats of formation and force field energies with their respective enthalpy ($\Delta\Delta H$) and energy (ΔE) differences between the two polymorphs of KAXXAI (All results in kcal mol⁻¹)

Method	AM1			PM3			Dreiding			Tripos		
	I	II	$\Delta\Delta H^a$	I	II	$\Delta\Delta H^a$	I	II	ΔE^a	I	II	ΔE^a
$\Delta H_f^{\text{cryst}}$	83.59	152.91	69.32	63.58	126.77	63.19	79.00	105.3	26.3	69.06	108.6	39.54
ΔH_f^1	-42.17	-40.45	1.72	-45.93	-44.55	1.38	40.79	44.65	3.86	-3.00	-2.16	0.84
ΔH_f^2	-43.76	-43.35	0.41	-47.30	-46.64	0.66	—	—	—	—	—	—
ΔH_f^3	-47.21	-46.08	1.13	-49.90	-49.17	0.73	—	—	—	—	—	—
ΔH_f^4	-48.38	-46.48	1.90	-50.03	-49.54	0.49	29.96	30.69	0.73	-11.80	-13.17	-1.37
ΔH_f^5	-48.46	-46.83	1.63	-51.53	-50.97	0.56	29.01	30.49	1.48	-14.00	-13.77	0.23
ΔH_f^6	—	—	—	—	—	—	30.84	32.38	1.44	-12.46	-12.01	0.45

^a $\Delta\Delta H = \Delta H_f(\text{form II}) - \Delta H_f(\text{form I})$, $\Delta E = E(\text{form II}) - E(\text{form I})$.

3.2.1 KAXXAI. The semi-empirical methods suggest that form I is the most stable, with AM1 and PM3 showing good agreement for all calculations. The same is true for the FF methods, except for Tripos ΔH_f^4 . This is in disagreement with the *ab initio* results which show that form II is slightly more stable. Using the ΔH_f^4 values, the semi-empirical and Dreiding methods show only a small energy difference between the two

forms, of between 1.90 (AM1) and 0.49 kcal mol⁻¹ (PM3) in favour of form I. Tripos favours form II by 1.37 kcal mol⁻¹. The ΔH_f^5 values (full optimisation) are very similar to these, and are consistent with the results of the force field cluster calculations, ΔH_f^6 . 6-31G** optimisations of all parameters except the two important torsions give relative energies (equivalent to ΔH_f^4). These show that form II is just under 1 kcal mol⁻¹ more stable

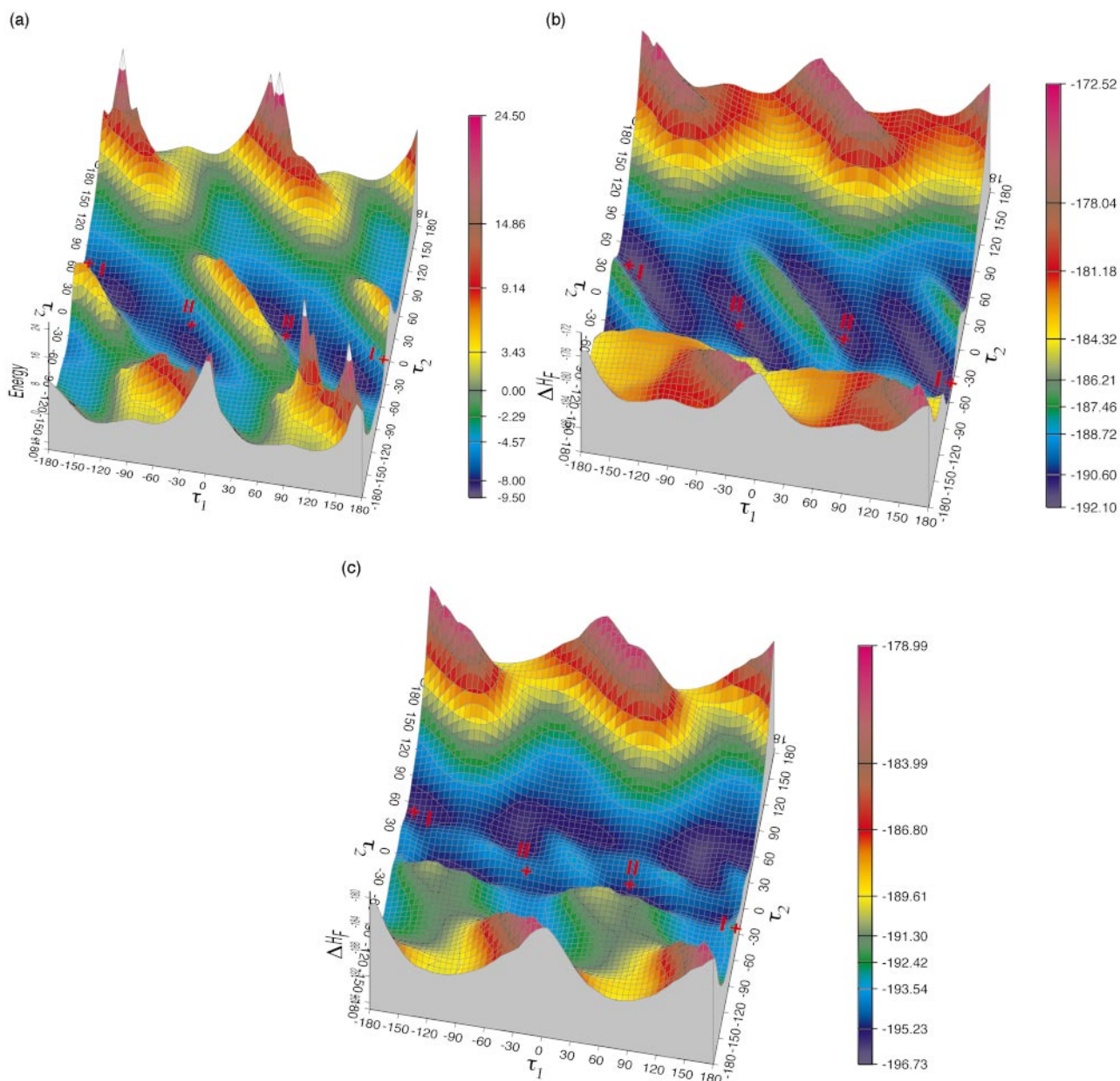


Fig. 7 (a) Force field, (b) AM1 and (c) PM3 potential energy surfaces for FPAMCA (energy in kcal mol⁻¹, torsions in degrees). Roman numerals indicate the location of forms I and II.

than form I. With the 3-21G basis set, this difference is 0.4 kcal mol⁻¹, still in favour of form II. Full optimisations to the nearest minima (equivalent to ΔH_r^5) give conformations with virtually the same energy.

3.2.2 BIXGIY. Generally, both AM1 and PM3 show that form III is the most stable, followed by form IV and then form I. The Tripos and Dreiding FF energy differences are again quoted relative to form III, although in this case, both methods tend to predict this to be the least stable form. We do not get a consistent ordering for the other two forms from the force field calculations. The *ab initio* calculations show neither consistency between basis sets nor in the ordering obtained from the different degrees of optimisation, although differences are very small. Apart from the FF results, the energy differences between forms are less than 2 kcal mol⁻¹, and care needs to be taken in drawing conclusions based upon such small values.

3.2.3 FPAMCA. Again, the tables show very little energy difference between the two forms. In the ΔH_r^4 calculations, all of the methods except PM3 agree that form II is more stable, by up to 2.7 kcal mol⁻¹ (Tripos) although the AM1 energy difference

is negligible. Full optimisations give virtually identical energies for both forms. The energy difference determined from the cluster calculations again show a slight stability in favour of form II. These energy differences are more in line with those calculated using the ΔH_r^4 values, as would be expected from structures that have been constrained by the surrounding molecules of the crystal lattice.

3.3 Optimised torsions

The optimised torsions obtained with all the theoretical methods are shown in Table 6.

3.3.1 KAXXAI. Both AM1 and PM3 produce optimised structures that differ in two ways from those found experimentally. Firstly, the nitrogen atom is calculated to be considerably more pyramidal than observed. Secondly, there is also deformation of the torsion defining the upper ring (τ_2), with optimised values of about 15° (AM1) and 30° (PM3). This part of the molecule is noticeably more planar in the observed crystal structures.

AM1 reproduces the torsions of KAXXAI form I very well, whereas the optimised value of τ_2 in form II differs by nearly

Table 3(a) Semi-empirical heats of formation with their respective enthalpy differences ($\Delta\Delta H$) between the three polymorphs of BIXGIY (All results in kcal mol⁻¹)

Method	AM1					PM3				
	I	III	IV	$\Delta\Delta H^a$	$\Delta\Delta H^b$	I	III	IV	$\Delta\Delta H^a$	$\Delta\Delta H^b$
$\Delta H_f^{\text{cryst}}$	87.60	71.15	110.75	16.45	39.60	59.12	45.49	79.96	13.63	34.47
ΔH_f^1	-18.62	-21.95	-22.82	3.33	-0.87	-34.97	-35.87	-36.67	0.90	-0.80
ΔH_f^2	-29.88	-30.46	-29.71	0.58	0.75	-41.68	-42.21	-41.81	0.58	0.40
ΔH_f^3	-33.65	-34.49	-33.80	0.84	0.69	-43.61	-44.81	-44.68	1.20	0.13
ΔH_f^4	-33.77	-34.67	-33.92	0.90	0.75	-43.68	-44.98	-44.85	1.30	0.13
ΔH_f^5	-34.04	-35.95	-35.95	1.91	0.00	-44.76	-45.78	-45.55	1.02	0.23

^a $\Delta\Delta H = \Delta H_f(\text{form I}) - \Delta H_f(\text{form III})$. ^b $\Delta\Delta H = \Delta H_f(\text{form IV}) - \Delta H_f(\text{form III})$.

Table 3(b) Force field energies with their respective energy differences (ΔE) between the three polymorphs of BIXGIY (All results in kcal mol⁻¹)

Method	Dreiding					Tripos				
	I	III	IV	ΔE^a	ΔE^b	I	III	IV	ΔE^a	ΔE^b
$\Delta H_f^{\text{cryst}}$	81.79	78.94	84.43	2.85	5.49	60.53	57.71	72.93	2.82	15.22
ΔH_f^1	42.79	41.47	39.73	1.32	-1.74	-5.70	-1.01	0.23	-4.69	1.24
ΔH_f^2	—	—	—	—	—	—	—	—	—	—
ΔH_f^3	—	—	—	—	—	—	—	—	—	—
ΔH_f^4	21.94	24.93	23.56	-2.99	-1.37	-20.36	-12.94	-12.89	-7.42	0.05
ΔH_f^5	21.86	24.08	21.86	-2.22	-2.22	-20.64	-16.82	-19.14	-3.82	-2.32
ΔH_f^6	25.56	26.13	24.09	-0.57	-2.04	-19.64	-14.44	-14.42	-5.20	0.02

^a $\Delta E = E(\text{form I}) - E(\text{form III})$. ^b $\Delta E = E(\text{form IV}) - E(\text{form III})$.

Table 4 Semi-empirical heats of formation and force field energies with their respective enthalpy ($\Delta\Delta H$) and energy (ΔE) differences between the two polymorphs of FPAMCA (All results in kcal mol⁻¹)

Method	AM1			PM3			Dreiding			Tripos		
	I	II	$\Delta\Delta H^a$	I	II	$\Delta\Delta H^a$	I	II	ΔE^a	I	II	ΔE^a
$\Delta H_f^{\text{cryst}}$	-102.24	-27.76	-74.48	-121.97	-55.78	-66.19	72.85	96.53	-23.68	54.32	94.62	-40.30
ΔH_f^1	-162.62	-171.46	8.84	-175.02	-183.03	8.01	53.01	52.73	0.28	9.41	6.11	3.30
ΔH_f^2	-186.46	-187.59	1.13	-191.23	-191.93	0.70	—	—	—	—	—	—
ΔH_f^3	-190.66	-190.99	0.33	-194.90	-193.80	-1.10	—	—	—	—	—	—
ΔH_f^4	-191.13	-191.42	0.29	-195.64	-194.56	-1.08	35.12	34.04	1.08	-4.41	-7.10	2.69
ΔH_f^5	-191.13	-191.53	0.40	-195.98	-195.54	-0.44	33.58	32.78	0.80	-7.74	-8.54	0.80
ΔH_f^6	—	—	—	—	—	—	35.80	34.62	1.18	-6.04	-7.99	1.95

^a $\Delta\Delta H = \Delta H_f(\text{form I}) - \Delta H_f(\text{form II})$, $\Delta E = E(\text{form I}) - E(\text{form II})$.

Table 5 Results of the *ab initio* calculations, with energies (au^a), optimised torsions (°) and relative conformational energies (kcal mol⁻¹)

Molecule	3-21G				6-31G**			
	E_{partopt}	E_{fullopt}	$\Delta E_{\text{partopt}}$	$\Delta E_{\text{fullopt}}$	E_{partopt}	E_{fullopt}	$\Delta E_{\text{partopt}}$	$\Delta E_{\text{fullopt}}$
KAXXAI	-1194.52143	-1194.52259	0.38	0.02	-1200.85837	-1200.86003	0.85	0.00
KAXXAI01	-1194.52204	-1194.52263	0.00	0.00	-1200.85973	-1200.86003	0.00	0.00
KAXXAI(30) ^b	—	-1194.52262	—	0.01	—	—	—	—
BIXGIY	-1210.42431	-1210.42450	1.91	1.80	-1216.86084	-1216.86115	0.00	0.00
BIXGIY02	-1210.42683	-1210.42737	0.33	0.00	-1216.85978	-1216.86096	0.67	0.12
BIXGIY03	-1210.42736	-1210.42737	0.00	0.00	-1216.85906	-1216.86096	1.12	0.12
BIXGIY(60) ^c	—	-1210.42736	—	0.01	—	—	—	—
FPAMCA	-1032.79960	-1032.80253	1.54	0.00	-1038.54242	-1038.54445	1.07	0.00
FPAMCA11	-1032.80206	-1032.80242	0.00	0.07	-1038.54412	-1038.54439	0.00	0.04

^a 1 au = 627.47237 kcal mol⁻¹. ^b Optimisation starting at $\tau_1 = 30^\circ$. ^c Optimisation starting at $\tau_1 = 60^\circ$.

20° from the value found in the crystal. The PM3 results show much larger differences for both forms, sometimes of over 40°.

Optimisation of form I using 3-21G fails to locate a minimum near either conformation, and the system descends to a minimum at about (-74, -5)°. The 6-31G** optimisations behave similarly, with optimised torsions of about (-82, -6)°. Thus both basis sets agree that there is a minimum with τ_2 approximately flat and τ_1 about 70–85°. The optimisations indicate a very shallow broad minimum exists on the PES, for which it is difficult to find the lowest energy point.

The FFs find two minima on the PES, with form I at about (45, 22)° and form II about (120, -15)°. Of the two FF methods the Dreiding results are the closer to the crystal torsions. The cluster calculations bring the torsions closer to those observed in the crystal structure reflecting the effects of crystal packing.

Overall, AM1 produces structures close to the two polymorphs. In contrast, optimisations of either form using PM3, 3-21G and 6-31G** locate only one minimum. The minima for these three methods are well removed from the torsions found in the crystal structures (Table 6). The FF approaches both

Table 6 Experimental and calculated torsions (°)

CSD Refcode		X-Ray	AM1	PM3	3-21G	6-31G**	Tripes	Dreiding	Cluster (Tripes)	Cluster (Dreiding)	
KAXXAI	I	τ_1	± 42.2	40.5	82.7	-71.4	-81.7	51.3	43.9	45.1	42.7
		τ_2	± 8.0	14.6	-27.7	-6.1	-5.9	21.9	22.0	14.6	11.0
KAXXAI01	II	τ_1	± 107.7	106.2	87.4	-77.5	-83.5	123.9	117.2	104.0	112.8
		τ_2	± 0.5	17.3	32.0	-4.4	-5.9	-20.6	-11.1	-1.8	-6.0
BIXGIY	I	τ_1	± 111.9	-111.0	-89.6	-109.2	-105.8	-121.9	-118.4	-117.6	-114.1
		τ_2	± 3.2	10.4	-25.1	-3.6	-7.7	6.2	3.6	-4.0	-2.9
BIXGIY02	III	τ_1	± 22.2	-55.3	-69.6	0.2	-58.0	-50.6	-36.2	-35.4	-20.6
		τ_2	± 0.7	7.1	21.7	-0.3	0.7	-5.1	-10.8	0.3	-2.1
BIXGIY03	IV	τ_1	± 0.6	55.4	-15.0	1.0	58.1	51.3	-36.4	-28.8	-0.8
		τ_2	± 1.1	-7.1	17.9	-0.1	-0.7	5.3	-10.5	10.5	0.8
FPAMCA	I	τ_1	± 176.5	154.9	144.7	-134.3	-133.6	-140.2	-151.5	-151.4	-169.1
		τ_2	± 37.1	27.6	60.4	11.3	13.4	28.0	29.8	22.7	33.4
FPAMCA11	II	τ_1	± 53.9	31.8	80.0	53.4	52.2	40.2	32.2	44.1	43.9
		τ_2	± 1.8	22.8	-30.3	10.4	12.9	29.7	29.7	19.4	9.4

locate two separate minima. The Dreiding results are closer to the crystal values and are of similar quality to the AM1 results.

3.3.2 BIXGIY. According to 3-21G, form I has final optimised torsions of $(-109, -4)^\circ$ close to the starting point. This agrees well with the 6-31G** calculations, which give optimised values of $(-106, -8)^\circ$. The 3-21G calculation on form III [initially $(22, 1)^\circ$] optimises to $(0, 0)^\circ$, and form IV optimises to $(1, 0)^\circ$, presumably the same minimum within the tolerance of the optimisation conditions. The same calculations performed with the 6-31G** basis set show radically different behaviour, with $\tau_1 \sim 58^\circ$ and τ_2 being planar for both forms III and IV.

Semi-empirical optimisations of all parameters show similar problems to those found for KAXXAI, with the nitrogen atoms being considerably more pyramidal than observed either experimentally or in the *ab initio* calculations. The second ring again twists out of the planar conformation by up to 10° for AM1 and 25° for PM3. Form I remains at the crystal conformation using AM1, but with PM3, τ_1 differs by about 20° . AM1 gives results very similar to 6-31G** for both forms III and IV, which optimise to around $(-55, 7)^\circ$, close to the global minimum on the AM1 surface. However, the two forms behave differently with PM3, with optimised values of $(-69, 22)$ and $(-15, 18)^\circ$, respectively.

The FF calculations show that Dreiding gives optimised torsions that are closer to the crystal structures than Tripes for all forms. It is interesting to note that Dreiding is the best of all methods at reproducing the crystal structure torsions found in form III (Table 6).

AM1, 3-21G and 6-31G** give optimised values that are very close to observed for form I but all fail to reproduce the conformation of form III. 3-21G is in good agreement for the planar form IV but AM1 and 6-31G** fail to reproduce this. In the case of AM1 this is presumably because the attractive $\text{CH}\cdots\text{N}$ interaction has not been well parameterised. It is perhaps surprising that 6-31G** is in closer agreement to the AM1 results rather than it is to 3-21G. PM3 does not give good results for any of the forms.

3.3.3 FPACMA. None of the methods predict a flat structure observed for the lower (trifluoromethyl substituted) ring ($\tau_1 \sim 180^\circ$) for form I. The differences between the crystal torsions $(-177, +37)$ and those from the *ab initio* calculations on form I are large. The two basis sets again give remarkably similar torsions of $(-134, +13)$ (6-31G**) and $(-134, +11)^\circ$ (3-21G). It is clear from the potential energy surfaces (Fig. 7) that the observed conformation of form I is a long way from the nearest minimum, and this explains why differences of 40° occur in τ_1 . In contrast, for form II, the *ab initio* methods are clearly superior in reproducing the torsions. All methods disfavour the planarity of the upper ring ($\tau_2 \sim 0^\circ$) found in the

crystal with the smallest differences being about 10° for the *ab initio* results. This might indicate that crystal packing forces overcome the torsional preferences of the molecule in the solid state to give some degree of planarity.

PM3 gives a poor reproduction of the torsions in both forms and also deviates significantly from the 6-31G** results. AM1 torsions are typically 20° out from those found in the crystal, and do not correlate particularly well with the 6-31G** results either. AM1 and PM3 suffer from the same pyramidalisation of the nitrogen found with BIXGIY and KAXXAI. Since this is not found in the *ab initio* structures, it is likely that this is a failing of the semi-empirical methods, rather than a true gas phase phenomenon.

As with virtually all the molecular orbital methods, the FF calculations give optimised torsions that are very different from those found in the crystal structures. In particular, the planar τ_2 in form II is over 30° out in the calculations. The form I torsions are also very different from those found in the solid state.

3.3.4 Summary of torsion results. Given the size of the systems studied, the best model we have for gas phase structures are the 6-31G** optimisations. We can compare the less time-consuming methods to these results to see if they give reliable structures at lower cost. For 3-21G, there is good agreement for most cases, with the exception being τ_1 of BIXGIY forms II and IV. Most of the methods would appear to concur with the 6-31G** prediction of a minimum of $\tau_1 \sim 55^\circ$, disfavouring the completely planar structure predicted by 3-21G (as observed in form IV).

The only AM1 structures to agree with those obtained from 6-31G** are those for the three forms BIXGIY. In both forms of the two other molecules, there is always at least one torsion that differs by over 20° . None of the PM3 torsions agree well with the 6-31G** results. As with AM1, the best results for the Tripes FF are for the three forms of BIXGIY, and the results for both forms of FPAMCA are reasonable. The Dreiding results are inferior to those from the Tripes FF.

It can be seen from this summary that the use of a single method to predict gas phase conformations is fraught with danger, as we have found in the past.⁴ Again, we recommend the use of large basis set *ab initio* optimisations backed up with a number of other studies to give confidence in the results.

3.4 Comparison of the one-dimensional torsion maps (τ_1) of KAXXAI, BIXGIY and FPAMCA

The PES maps indicate that the low-lying region where $|\tau_2| < 90^\circ$ (in which there is a $\text{NH}\cdots\text{O}$ intramolecular hydrogen bond present) will be by far the most highly occupied portion of the PES. This is confirmed by the diarylamine CSD search. To investigate this further, one-dimensional AM1 scans of τ_1 for **1**, **2** and **3** are superimposed in Fig. 8. In this case, τ_2 has been

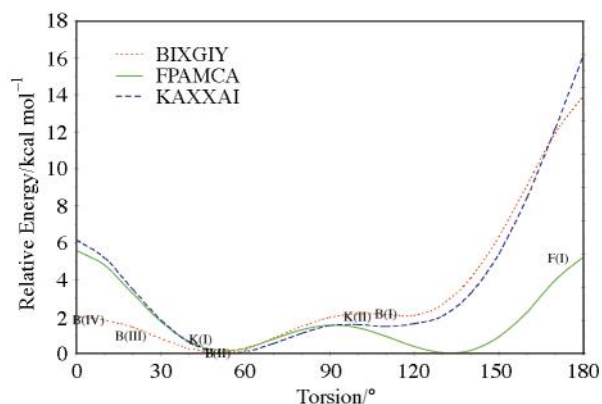


Fig. 8 AM1 One-dimensional torsional scans (τ_1) for KAXXAI, BIXGIY and FPAMCA.

fixed at 0° , so the plot is an actual slice through the two-dimensional surfaces, and minima do not necessarily correspond to those found in those in Table 6 in which τ_2 can also twist. As would be expected, the scans show that in FPAMCA, where there is no methyl group *ortho* to the amine nitrogen, the barrier at 180° is much lower. As a consequence, a planar conformation ($\tau_1 = 180^\circ$) is more likely for FPAMCA, and indeed a polymorph is observed in which $\tau_1 = \pm 176.5^\circ$. However, steric constraints mean that the two rings cannot be coplanar, forcing τ_2 to deviate from planarity in this structure.

The curves for KAXXAI and BIXGIY both show very shallow minima at $\sim 110^\circ$, and both have polymorphs associated with this conformation. There is no equivalent polymorph reported for FPAMCA at this position, or indeed at the nearby minimum at $\sim 130^\circ$. The conformational profile shows that there are no energetic reasons why this conformation should not be found and perhaps one of the six polymorphs of this molecule that have not had their crystal structure determined could have this torsion.²⁵

The geometry at 110° would appear to be a subtle balance of electronic effects driving the torsion away from 90° and a steric clash between the methyl group and the upper ring driving the torsion away from 180° , as shown schematically in Fig. 9. The absence of this methyl group in molecule **3** removes most of the steric part of the energy, and this moves the minimum to a higher torsion and increases its relative stability. The pattern of polymorphs at this torsion suggest that even narrow gas phase minima can be important in determining the observed crystal chemistry.

Both **1** and **3** exhibit minima and reported polymorphs at around 50° . There is also a minimum at this torsion for BIXGIY, but none of the reported polymorphs considered here have this torsion. § BIXGIY exhibits a polymorph at 22° , which is not a stationary point on the AM1 plot (none of the optimisations of this form locate a nearby minimum). Thus, it is apparent that crystal structure conformations do not necessarily have to occur at minima on the gas phase PES. The only molecule to have a polymorph at $\tau_1 = 0^\circ$ is BIXGIY (form IV), which is a maximum on all except the 3-21G surface.

3.5 Alternative minima

In the moderately high-lying $|\tau_2| > 90^\circ$ region, the FF and AM1 maps of all three molecules show either minima or flat regions of the surface which require further characterisation. These regions are within 8–10 kcal mol⁻¹ of the global minima. To investigate these further, full optimisations have been

§ It is interesting to note that the zwitterionic polymorph (BIXGIY04) has a value of τ_1 of about 40° , however, the electronic structure of this form means that the torsional map could be very different from the one presented here.

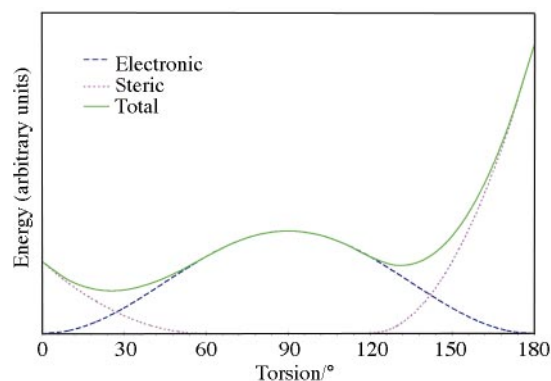


Fig. 9 Generic representation of the energy components of τ_1 for **1** and **2**.

performed using AM1 and the Tripos FF (with AM1 charges calculated at the geometry of the first polymorph in each case), starting at both $(-140, -140)$ and $(40, -140)^\circ$. The optimised torsions and energies are shown in Table 7. The structures do not descend to the low energy central valley, and locate minima in the higher energy $|\tau_2| > 90^\circ$ region.

For KAXXAI, the minima are 7.3 and 9.4 kcal mol⁻¹ less stable than the AM1 global minimum, or about 6 kcal using the FF. The difference for the lower of the minima of BIXGIY is 8.4 (AM1) or 6.2 kcal mol⁻¹ (FF). For FPAMCA, these numbers are 6.7 (AM1) and 5.6 kcal mol⁻¹ (FF). All of these minima are within the previously determined energy window of about 10 kcal mol⁻¹ we have previously found between polymorph conformations. Thus, any one of these conformations could be a viable basis for as yet undiscovered polymorphs.

Fig. 10 shows FF structures for KAXXAI representing the alternative minima located from optimisations started at $(-140, -140)$ and $(40, -140)^\circ$. Corresponding structures for BIXGIY and FPAMCA have similar geometries and therefore have not been shown. It appears that these minima do not have the intramolecular $\text{NH} \cdots \text{O}$ hydrogen bond observed in the crystal structures, and this accounts for the higher energies of these structures. However, the carboxylic acid group is still available to form intermolecular COOH dimers, as frequently observed in this type of compound, although it is hard to see how the loss of the $\text{NH} \cdots \text{O}$ hydrogen bond can be compensated for by additional lattice contributions to give a stable crystal.

From the conformational maps, it can be seen that the structures lie in reasonably broad minima with a very small barrier separating them from the $\tau_2 \sim 0$ structures. These minima seem to result from a subtle balance of the stabilising effect of a planar conformation and the steric repulsion of approaching groups, similar to that depicted in Fig. 9.

3.6 Lattice energy calculations

Overall, the differences between observed and Dreiding optimised structures are very small. The mean change in the cell lengths is 0.17 Å (the maximum being a 0.45 Å change in the BIXGIY value of a). The mean change in the cell angles is 1.39° (the maximum being a 5° change in a for BIXGIY03).

3.6.1 KAXXAL. Lattice energy calculations employing the Dreiding force field (Table 8) indicate that form I packs 1.4 kcal mol⁻¹ more efficiently than form II. However, the Tripos FF and minimised Dreiding calculations imply the structures are of equal stability. The experimental heats of fusion are given as 11.57 (I) and 10.16 kcal mol⁻¹ (II) and the liquid phases have been shown to be identical.²⁵ This indicates that form I is 1.4 kcal mol⁻¹ more stable than form II, in good agreement with the Dreiding calculations. The melting points are 214.5 and

Table 7 AM1 and Tripos FF optimised energies and torsions ($^{\circ}$) of the minima located in the higher-lying regions ($|\tau_2| > 90^{\circ}$) of the PESs

	AM1			Tripos FF		
	KAXXAI	BIXGIY	FPAMCA	KAXXAI	BIXGIY	FPAMCA
$\tau_1^{(40,140)}$	-38.7	26.4	-30.6	29.9	35.3	18.0
$\tau_2^{(40,140)}$	-87.8	-109.8	-96.2	-129.5	-139.2	-117.7
Energy ^a (40,140)	-41.2	-27.6	-184.8	-8.2	-14.4	-2.7
$\tau_1^{(-140,-140)}$	-111.6	-116.4	-153.7	-139.0	-137.0	-159.0
$\tau_2^{(-140,-140)}$	-121.7	-120.5	-115.3	-136.6	-142.0	-122.0
Energy ^a (-140,-140)	-39.1	-26.3	-184.8	-8.0	-14.3	-2.9

^a Energies in Kcal mol⁻¹.

Table 8 Lattice energy calculations using the Tripos and Dreiding force fields in kcal mol⁻¹

Refcode	Form	Tripos ^a	Dreiding ^a	Dreiding ^b	Dreiding ^c
KAXXAI	I	-29.5	-28.1	-34.0	-34.5
KAXXAI01	II	-29.2	-26.7	-34.3	-34.5
BIXGIY	I	-25.5	-9.3	-31.1	-32.3
BIXGIY02	III	-28.1	-28.2	-35.3	-35.5
BIXGIY03	IV	-28.1	-24.6	-30.6	-35.5
FPAMCA	I	-28.1	-27.7	-33.8	-33.9
FPAMCA11	II	-28.0	-30.6	-34.0	-34.3

^a Single point lattice energies. ^b Lattice energy minimisation, with rigid body rotation and translation (unit cell fixed). ^c Full rigid body minimisation including relaxation of rotation, translation and unit cell parameters.

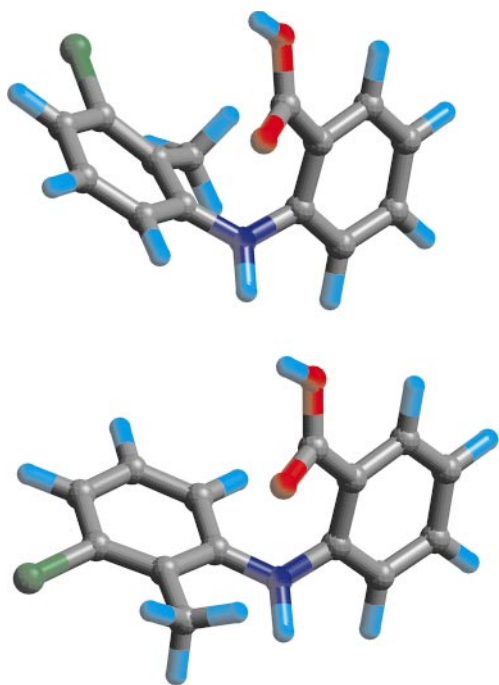


Fig. 10 Force field minimised structures from the alternative minima found on the KAXXAI surface at $(-140, -140)^{\circ}$ (top) and $(40, -140)^{\circ}$ (bottom).

210.9 $^{\circ}\text{C}$ respectively, being in line with the ordering expected from the heats of fusion and the densities (Table 1).

3.6.2 BIXGIY. Dreiding lattice energy calculations predict that form I is dramatically less stable than forms III and IV. This contradicts the other calculations, and it is likely that this is a consequence of a failing of the Dreiding force field, which has problems in the treatment of carboxylic acid dimers.²⁴ Variations in the results mean that it is not evident which form of BIXGIY has the most stable lattice. Differential thermal analysis of the polymorphs indicates that forms III and IV are transformed into form I at 156 and 144 $^{\circ}\text{C}$, respectively, which then melts at 242 $^{\circ}\text{C}$.²⁶ This would imply that form I is the most stable, at least at these elevated temperatures. However, it

is not possible to comment on the relative room temperature stabilities.

3.6.3 FPAMCA. Dreiding lattice energy calculations predict that form II is 2.9 kcal mol⁻¹ more stable than form I, but the two forms are equally stable using the Tripos FF or the minimised Dreiding approach. These calculations are consistent with the observed densities, but are at odds with the melting points 128 (form II) and 134 $^{\circ}\text{C}$ (form I).²⁵

4 Polymorph prediction studies

The conformational map shown in Fig. 8 forms the basis for polymorph prediction studies. These involved placing molecules of either BIXGIY, KAXXAI or FPAMCA into the lattice arrangements of one of the other two molecules to produce as yet unobserved packing motifs. Rigid body lattice energy minimisation techniques were used to determine the relative stabilities of these postulated structures. Two minimisation strategies were employed in an attempt to push the minimisation past local minima. Firstly, the molecular rotations and translations were allowed to relax in a fixed unit cell followed by a subsequent minimisation in which the cell parameters were also allowed to move. Secondly, all the parameters (cell and molecular degrees of freedom) were allowed to relax from the start of the minimisation. Only the most stable arrangements are quoted. The molecular conformation was held fixed at the input values and the charges used were those from the AM1 method as described previously. The results are reported in Table 9.

At $\tau_1 \sim 50^{\circ}$, polymorphs are seen for both KAXXAI and FPAMCA [K(I) and F(II)]. This is a minimum for all three structures but no polymorph is observed at this conformation of BIXGIY. The conformation of BIXGIY form III was introduced into the lattices of KAXXAI form I (TRIAL 1) and of FPAMCA form II (TRIAL 2). These structures were then minimised producing packing energies of -30.7 and -31.9 kcal mol⁻¹, respectively. A comparison with the fully minimised lattice energies (Table 8) shows that neither of the two trial structures are as stable as the observed forms. The TRIAL 2 structure is close in energy to the value found for form I BIXGIY and on the limit of the energy window suggested for possible polymorphs.⁷ It is suggested in the literature that the

Table 9 Lattice energies (kcal mol⁻¹), cell parameters^a and densities for predicted polymorphs

Structure	τ_1 conformation from	Packing motif from	Lattice energy ^b	$a/\text{\AA}$	$b/\text{\AA}$	$c/\text{\AA}$	β°	Density/ Mg m ⁻³		
Trial 1	BIXGIY	III	KAXXAI	I	-30.7	13.78	7.37	13.15	78.83	1.332
Trial 2	BIXGIY	III	FPAMCA	II	-31.9	3.85	22.29	14.60	95.66	1.399
Trial 3	BIXGIY	I	KAXXAI	II	-33.6	4.36	33.31	8.52	103.78	1.450
Trial 4	KAXXAI	I	FPAMCA	II	-33.4	10.08	8.57	15.00	101.69	1.369
Trial 5	FPAMCA	II	KAXXAI	I	-30.8	4.50	32.28	9.30	102.93	1.418
Trial 6	BIXGIY	III ^c	KAXXAI	I	-33.1	3.99	21.99	14.14	88.25	1.408
Trial 7	BIXGIY	III ^c	FPAMCA	II	-31.2	15.42	8.00	10.69	86.11	1.327
Trial 8	FPAMCA	I ^c	KAXXAI	II	-31.3	4.73	40.16	9.45	46.96	1.425
Trial 9	FPAMCA	I ^d	KAXXAI	II	-26.6	4.46	38.03	8.27	105.58	1.384

^a Space group $P2_1/c$. ^b Dreding lattice energy reported is lowest found from minimisation strategies (see text). ^c τ_1 rotated to nearest AM1 minimum value (see text). ^d τ_1 rotated to 134° (see text).

packing energy of potential polymorphs should be within 10% of the most stable form.

In a second set of predictions, the packing of KAXXAI (form II) and BIXGIY (form I) were examined and predictions carried out, for which $\tau_1 \sim 110^\circ$. It is important to stress that even though these two molecules have very similar torsion values they pack in very different ways. BIXGIY (I) utilises the aromatic nitrogen to form O-H...N interactions rather than the traditional carboxylic acid dimer (seen in BIXGIY forms III and IV and KAXXAI form II). This has already been discussed and illustrated in Figs. 1–3. BIXGIY (I) was therefore introduced into the KAXXAI (II) lattice and forced to pack in the conventional carboxylic acid dimer. This structure (TRIAL 3) is actually more stable (-33.6 kcal mol⁻¹) than the observed form I (-32.3 kcal mol⁻¹). This is a surprising result for two reasons: (i) the TRIAL 3 packing is not observed in the reported crystal structures, and (ii) the difference in stability is likely to be an underestimate given that the Dreding force-field tends to underestimate the strengths of carboxylic acids and hence bias against their packing.²⁴ The alternative packing arrangement (*i.e.* KAXXAI form II in BIXGIY form I) is not possible because KAXXAI does not contain the appropriate functionality to form the O-H...N interactions. The packing arrangement for TRIAL3 is shown in Fig. 11 in a view that can be compared directly with Fig. 1(b) (KAXXAI form II).

In another set of calculations the KAXXAI (I) and FPAMCA (II) molecules and lattices were interchanged producing structures TRIAL 4 and TRIAL 5. Neither of the interchanged structures were as stable as the observed forms. However, for KAXXAI in the FPAMCA lattice, the energy difference was around 1 kcal mol⁻¹, which is within 10% of the most stable form of KAXXAI. The fact that it is not observed is in this case less of a surprise than for TRIAL3 (compared to BIXGIY I). Here, a more stable alternative packing arrangement is available at the same value of τ_1 .

The next set of calculations used conformations in which τ_1 had been rotated to the value found in the nearest AM1 minimum. Structure TRIAL 6 took the BIXGIY III conformation, rotated τ_1 to 55.4° and packed it into the lattice of KAXXAI I. This structure has a more stable lattice energy than form I, and hence it is quite possible that it could occur. The same conformation packed into the lattice of FPAMCA II constitutes structure TRIAL 7. This lattice is not within 10% of the most stable form.

TRIAL 8 uses the conformation found in FPACMA I with τ_1 rotated to the AM1 minimum from Fig. 8 (134°) and τ_2 left at the crystal structure value and packed into the lattice of KAXXAI II. This motif is based upon a conformation of KAXXAI with $\tau_2 = 0^\circ$, thus a similar study (TRIAL 9) was performed, except τ_2 was set to zero. Neither trial gives packing motifs approaching the stability of the observed forms.

The crystal structure details reported in Table 9 show that the calculated densities of the predicted polymorphs are lower than the experimentally derived values reported in Table 1. This is

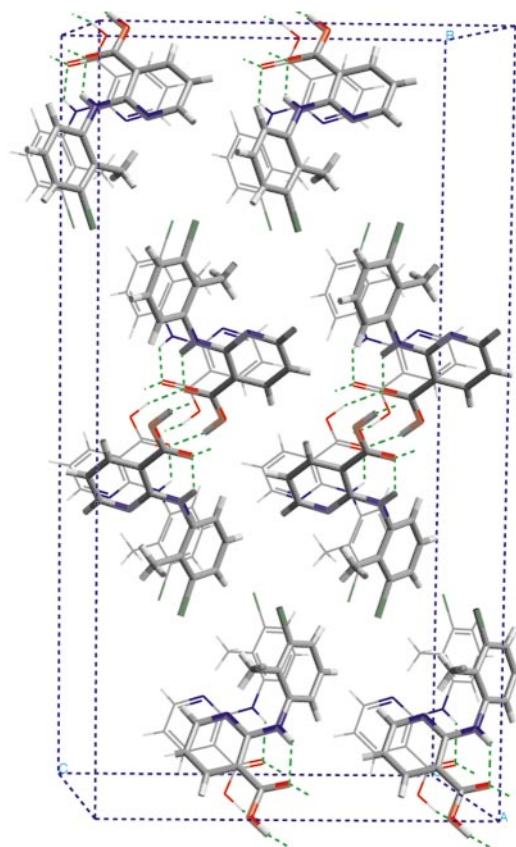


Fig. 11 Crystal packing of the stable proposed 'novel polymorph' of BIXGIY (TRIAL 3).

believed to be a consequence of the Dreding force field description of the hydrogen bonding. It has been shown recently that for the Dreding force field the intermolecular hydrogen bonds between carboxylic acid groups are too long.²⁴ Therefore it would be expected that densities calculated using this approach (and those from the fully minimised structures) will be lower than those observed experimentally. The cell parameters reported for each of the trials in Table 9 show that the most stable predicted polymorphs, TRIALS 3 and 6, involve only small distortions of the crystal lattice. However, some of the other trials undergo a large distortion of the crystal lattice during minimisation. In these cases, the resultant packing arrangements are predicted to be less stable than the known polymorphic forms.

5 Discussion

A number of theoretical methods have been employed to investigate the gas phase potential energy surfaces for three diarylamines. Although there is general consistency between

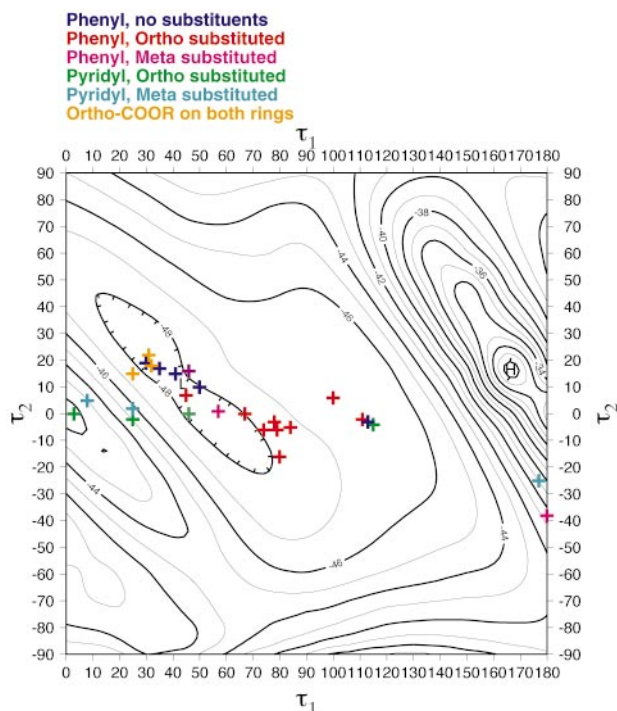


Fig. 12 Torsional distribution of diarylamines found in the CSD superimposed on the AM1 potential energy surface of KAXXAI (energy in kcal mol⁻¹, torsions in degrees).

the methods, the fine detail of the low-lying regions varies from method to method. In particular, there are differences in the number, location and relative energies of the minima on the PES. As found previously,⁴ PM3 appears to be less suitable for the type of study described here.

In general, the observed polymorphic conformations are located at, or near to, minima on the calculated conformational surfaces. However, one of the polymorphs of BIXGIY occurs at a maximum, whilst another is located between this point and a minimum. One of the forms of KAXXAI lies in a region of the PES that has a low gradient, but is not unambiguously characterised as a minimum (at $\tau_1 \sim 110^\circ$). There are also some significant differences between the gas phase optimised minima and the observed conformations in the solid state. In addition, there are several reasonably low-lying minima on the PES that are not occupied by observed polymorphs. These features increase the difficulty in the prediction of polymorphs.

One of the key features in all the potential surfaces is that the low lying regions cover a wide range of τ_2 values. The spread is much larger than that found from our analysis of related molecules in the CSD. To illustrate this, in Fig. 12, we have superimposed the observed torsions from Fig. 4 on the AM1 potential energy surface for KAXXAI. This has been chosen as being a generally representative PES for diarylamines, but is not necessarily characteristic of each individual molecule. It can be seen that apart from a small cluster of mixed compounds in the minimum at $\tau_1 \sim 110^\circ$, a large proportion of the compounds lie in or near the global minimum. Nearly 80% of the observations lie within 2 kcal mol⁻¹ of the global minimum energy. However, this energy cut off covers a large region of conformational space, most of which is not occupied by observed crystal structures. In particular, there are very few deviations from $\tau_2 \sim 0$. The lack of observed crystal structures in this region and in the low-lying alternative minima could be a consequence of the inability to pack these conformations in a stable lattice, or more likely, an underestimation of the energy needed to break the CO...NH hydrogen bond by AM1. Indeed, an HF/6-31G** optimisation with both τ_1 and τ_2 frozen at $+40^\circ$ gives a structure that is nearly 8 kcal mol⁻¹ higher than the minimum for this value of τ_2 ($\tau_1 \sim -20^\circ$). The corresponding AM1 energy differ-

ence is only 1 kcal mol⁻¹. This emphasises the need to employ a range of theoretical methods to check for consistency when attempting this type of study.

In Fig. 12, the *o*-substituted phenyl compounds (red) cluster at $\tau_1 \sim 70^\circ$. Since the torsional map is representative of this type of compound, it is surprising that these compounds are geometrically removed from the global minimum. However, there is very little energy difference between this cluster and the minimum. The molecule QQBTY01 introduces a special problem for those interested in polymorph prediction because it has two molecules in the asymmetric unit, with τ_1 values of 46.6 and 110.0°. Thus both minima from the KAXXAI and BIXGIY surfaces are occupied in the same crystal.

In a recent study, it was shown that torsion angles associated with high strain energy (>1 kcal mol⁻¹) appear to be very unusual in crystal structures,⁵ and it was concluded that crystal packing effects rarely have a strong systematic effect on molecular conformations. In general, our calculations indicate that the typical energy differences seem to be about 2 kcal mol⁻¹. Calculations of energy differences in polymorphs are not without difficulty. Our highest level of calculations (6-31G**) suggests that the maximum energy differences are around 1 kcal mol⁻¹ but our equivalent force field and semi-empirical calculations suggest energy differences to be slightly higher, at around 3 and 2 kcal mol⁻¹ respectively. However, in some individual cases, certain methods predict larger energy differences.

Fig. 8 shows the AM1 torsional energy profiles for the three molecules studied here. This map is equivalent to a one-dimensional slice taken through Fig. 12 at $\tau_2 = 0$. It is worth noting that the greatest population of known crystal structures occurs between the 30–90° region which coincides with a minimum for all three torsional profiles (Fig. 8). Using these profiles and the observed packing for the known polymorphs, it was possible to suggest alternative packing motifs. Rigid body lattice energy minimisation was employed to examine the relative stability of these postulated packing motifs. In general, all motifs gave reasonably stable structures. In some cases, the postulated motifs were within the accepted energy window for the observation of polymorphic forms. In one case (TRIAL 6), the predicted motif was more stable than the least stable observed polymorph. We have also predicted a packing motif (TRIAL 3) which has the same conformation as, but is more stable than the observed polymorph (BIXGIY I).

It has been recently demonstrated that from known crystal structures of a polymorphic material, it is possible to rationalise the effect of solvent on crystal growth and nucleation and hence the polymorphic outcome of a crystallisation experiment.²⁷ The basis of this strategy is a complete knowledge of the packing motifs of the observed form. In this paper, we have shown methods for predicting structural information on potential polymorphs that are as yet unobserved. Clearly this information can form the basis for an experimental investigation to generate these predicted polymorphs.

6 Conclusions

Ab initio polymorph prediction remains an admirable long-term scientific goal. Previous papers have demonstrated the difficulties in packing rigid molecules to give polymorph predictions. In this work, we have demonstrated the added complexity introduced by molecules with even a small number of conformational degrees of freedom. These difficulties arise from the following factors: (i) Observed crystal structure conformations occur at minima, maxima and non-stationary points on the gas phase potential energy surface. This makes the use of gas phase minimised structures as input into crystal structure prediction techniques somewhat questionable; (ii) Not all low energy minima on the calculated potential energy surfaces are occupied by observed crystal structures; (iii) Even observed structures that lie in minimum energy regions of the

gas phase surface are often structurally quite different from the lowest energy point of that minimum. Considerable torsional differences have been observed; (iv) Most of the observed structures occur within a few kcal mol⁻¹ of the gas phase minimum. However the conformational extent of this energy contour is much larger than the distribution of related crystal structures. In particular, a larger range of τ_2 values might be expected from the surface maps than is seen experimentally.

In this paper, we have demonstrated a rational approach to polymorph elucidation using a combination of theoretical calculations and crystallographic informatics. We have postulated alternative packing motifs based on our knowledge of the potential energy surfaces, the experimental distribution of torsions and their observed packing arrangements. The result is a number of predicted packing arrangements that are within the conventionally accepted range of lattice energy differences. One of these forms is predicted to be more stable than the observed form found at the same position on the potential energy surface.

References

- 1 J. Bernstein and A. T. Hagler, *J. Am. Chem. Soc.*, 1978, **100**, 673.
- 2 J. J. Wolff, *Angew. Chem., Int. Ed. Engl.*, 1996, **35**, 2195.
- 3 G. R. Desiraju, *Crystal Engineering – The Design Of Organic Solids*, Elsevier, Amsterdam, 1989.
- 4 D. Buttar, M. H. Charlton, R. Docherty and J. Starbuck, *J. Chem. Soc., Perkin Trans. 2*, 1998, 763.
- 5 F. H. Allen, S. E. Harris and R. Taylor, *J. Comput.-Aided Mol. Des.*, 1996, **10**, 247.
- 6 H. R. Karfunkel and R. J. Gdanitz, *J. Comput. Chem.*, 1992, **13**, 1771.
- 7 A. Gavezzotti, *J. Am. Chem. Soc.*, 1991, **113**, 4622.
- 8 F. H. Allen, O. Kennard and R. Taylor, *Acc. Chem. Res.*, 1983, **16**, 146.
- 9 K. Vilbour Andersen, S. Larsen, B. Alhede, N. Gelting and O. Buchardt, *J. Chem. Soc., Perkin Trans 2*, 1989, 1443.
- 10 M. Takasuka, H. Nakai and M. Shiro, *J. Chem. Soc., Perkin Trans. 2*, 1982, 1061.
- 11 J. F. McConnell, *Cryst. Struct. Commun.*, 1973, **3**, 459.
- 12 H. M. Krishna Murthy, T. N. Bhat and M. Vijayan, *Acta Crystallogr., Sect. B*, 1982, **38**, 315.
- 13 SYBYL Molecular Modelling Software, Tripos Inc., 1699 S. Hanley Rd., St. Louis, MO, USA.
- 14 MOPAC93, QCPE program 455. Quantum Chemistry Program Exchange (QCPE), Creative Arts Building 181, Indiana University, Bloomington, Indiana 47405.
- 15 M. J. S. Dewar, E. G. Zoebisch, E. F. Healy and J. J. P. Stewart, *J. Am. Chem. Soc.*, 1985, **107**, 3902.
- 16 J. J. P. Stewart, *J. Comput. Chem.*, 1989, **10**, 209.
- 17 GAMESS-UK is a package of *ab initio* programs written by M. F. Guest, J. H. van Lenthe, J. Kendrick, K. Schoffel, P. Sherwood and R. J. Harrison, with contributions from R. D. Amos, R. J. Buenker, M. Dupuis, N. C. Handy, I. H. Hillier, P. J. Knowles, V. Bonacic-Koutecky, W. von Niessen, V. R. Saunders and A. Stone. The package is derived from the original GAMESS code due to M. Dupuis, D. Spangler and J. Wendoloski, NRCC Software Catalogue, Vol. 1, Program No. QG01 (GAMESS), 1980.
- 18 S. L. Mayo, B. D. Olafson and W. A. Goddard III, *J. Phys. Chem.*, 1990, **94**, 8897.
- 19 CERIOUS Molecular Modelling Software, MSI, Cambridge, UK.
- 20 J. Baker, *J. Comput. Chem.*, 1986, **7**, 385.
- 21 W. H. F. Smith and P. Wessel, *Geophysics*, 1990, **55**, 293.
- 22 R. Docherty, K. J. Roberts and G. Clydesdale, *J. Crystal Growth*, 1996, 166, 78. HABIT95, QCPE program 670. Quantum Chemistry Program Exchange (QCPE), Creative Arts Building 181, Indiana University, Bloomington, Indiana 47405.
- 23 A. I. Kitaigorodski, *Molecular Crystals And Molecules*, Academic Press, New York, 1973.
- 24 R. Payne, R. Roberts, R. Rowe and R. Docherty, *J. Comput. Chem.*, 1998, **19**, 1.
- 25 A. Burger and R. Ramberger, *Microchim. Acta*, 1979 II, 273.
- 26 M. Takasuka, H. Nakai and M. Shiro, *J. Chem. Soc., Perkin Trans 2*, 1982, 1061.
- 27 N. Blagden, R. J. Davey, H. F. Leiberman, L. Williams, R. Payne, R. Roberts, R. Rowe and R. Docherty, *J. Chem. Soc., Faraday Trans.*, 1998, **94**, 1035.

Paper 8/09462D